J. Membrane Biol. 52, 147–159 (1980)

The Journal of
Membrane Biology

Structural and Functional Membrane Polarity in Cultured Monolayers of MDCK Cells

Marcelino Cereijido*, Jordi Ehrenfeld, Isaura Meza, and Adolfo Martínez-Palomo
Departments of Physiology and Cell Biology, Centro de Investigación y de Estudios Avanzados del I.P.N., México 14, D.F., México

Summary. MDCK cells form monolayers which have many of the properties usually found in transporting epithelia. The present article is devoted to the study of the structural and functional polarization of MDCK cells, which is one of the central features of transporting epithelia. The results show: (i) that MDCK monolayers transport 2.6 μmol hr^{-1} cm^{-2} of sodium in the apical to basolateral direction; (ii) the passive flux of this ion is relatively large (20.3 mole hr^{-1} cm^{-2}), which is a characteristic of leaky epithelia; (iii) a large fraction of the penetration of sodium into the cells proceeds through an amiloride-sensitive channel, and the exit is operated mainly by a ouabain-sensitive pump; (iv) the net transport of sodium from the apical to the basolateral side agrees with the asymmetric labeling of the pumps with ^{3}H-ouabain; (v) this asymmetric labeling agrees, in turn, with a higher concentration of intramembrane particles (IMPs) in freeze-fracture replicas of the basolateral side of the plasma membrane; (vi) the structural polarization of confluent MDCK cells is also revealed by the location of microvilli, occluding junctions, and pinocytotic vesicles; and (vii) the presence of a continuous ring formed by actin microfilaments visualized by immunofluorescence under the lateral aspect of the plasma membrane that may be related to the distribution of the occluding junctions, which act as barriers separating apical from basolateral membrane components.

In natural epithelia, like the amphibian skin and the vertebrate gallbladder, net transport of substances is the consequence of two main properties of epithelial cells: (i) they contact each other to form occluding junctions (tight junctions) which confer to the cell layer the role of an effective permeability barrier (Erlij & Martínez-Palomo, 1978), and (ii) they are polarized, i.e., channels, carriers, pumps, and hormonal receptors present on the basolateral membrane region, are different from those on the apical side. These two properties have also been observed in monolayers of MDCK cells (Leighton *et al.*, 1969; Misfeldt, Hamamoto & Pitelka, 1976; Cereijido *et al.*, 1978). Studies of passive ionic permeabilities, electrical parameters, distribution of lanthanum and peroxidase, and freeze-fracture electron microscopy have shown that these monolayers resemble leaky epithelia, where most of the passive permeation proceeds through a paracellular pathway (Machen, Erlij & Wooding, 1972; Martínez-Palomo & Erlij, 1973). Since this pathway is limited at the apical side by a tight junction, the information collected provides a consistent picture of the properties of its strands. On the contrary, the information available on the second characteristic of the cells of transporting epithelia, i.e., their structural and functional polarization, is relatively scarce in MDCK monolayers, and therefore in the present study we have concentrated our attention on this aspect. To this purpose, we have combined the study of tracer fluxes, ^{3}H-ouabain-binding, and freeze-fracture electron microscopy of plasma membranes. The results indicate that: (i) MDCK monolayers transport a net amount of sodium from the apical to the basolateral side. Their cells possess mechanisms similar to those present in certain natural epithelia, e.g., a passive flux of Na into the cells, which is sensitive to amiloride, and an active extrusion carried out by a ouabain-sensitive pump; (ii) the Na pumps are concentrated on the basolateral side; (iii) this concentration of Na pumps is matched by a higher density of intramembrane particles (IMPs) on the basolateral side of MDCK plasma membranes in

* *Address for reprint requests:* Department of Physiology, Centro de Investigación y de Estudios Avanzados del I.P.N., Apartado Postal 14-740, México 14, D.F., México.

0022-2631/80/0052-0147 $02.60

comparison to the apical one; and (iv) we have studied the distribution of microtubules and microfilaments in these monolayers using monospecific antibodies and immunofluorescence microscopy. Actin filaments were found to form a continuous ring under the region of the plasma membrane where the cells make occluding junctions with adjacent cells. This observation agrees with the view that the cytoskeleton is involved in the topographical distribution of membrane components (Nicholson, 1976; Ash, Louvard & Singer, 1977; Koch & Smith, 1978) and with the permeability of the occluding junctions (Bentzel *et al.*, 1976; Meza *et al.*, 1978).

Materials and Methods

Cell Culture

MDCK (*M*adin, *D*arby, *C*anine, *K*idney) cells constitute an established line obtained in 1958 by Madin and Darby from the kidney of a normal cocker spaniel female dog. When grown on a nonpermeable support (i.e., a Petri dish) the cells form monolayers with blisters attributed to unidirectional water transport (Leighton *et al.*, 1969). The cells in the 100 to 110th passages were grown at 36.5 °C in roller bottles with an air-5% CO_2 atmosphere and 100 ml of complete Eagle's Minimal Essential Medium (CMEM) with Earle's salts (Grand Island Biological Col. (GIBCO F-11), 100 U/ml of Penicillin, 100 µl/ml of streptomycin and 10% calf serum (GIBCO 617). Cells were harvested with trypsin-EDTA (GIBCO 540), and plated on 30-mm Petri dishes (Lux Scientific Corp., Thousand Oaks, Calif.) or on disks of a Nylon cloth (HC-103 Nitex, Tetko, Inc., Elmsford, N.Y.) coated with collagen extracted from rat tails by the method of Bornstein. Once sterilized under UV light, each disk was placed into a 16-mm well of a multichamber dish (Limbro Chemical Co., New Haven, Conn.), and a suspension of MDCK cells in 1.0 ml of CMEM was added to a density of 4×10^5 cells/cm^2. After incubation for 90 min at 36.5 °C in an air-5% CO_2 atmosphere with constant humidity (V.I.P. CO_2 Incubator 417, New Brunswick, N.J.) to allow for attachment of the cells, disks were transferred to another multichamber dish containing fresh CMEM without cells. A continuous monolayer is thus formed which starts to develop a measurable electrical resistance across in some 5 hr, and reaches a steady value in about 20–24 hr (Cereijido *et al.*, 1978). All monolayers used in the present study have been confluent for more than two days.

Na Fluxes Across the Monolayer of MDCK Cells

Disks containing monolayers were mounted as flat sheets between two Lucite chambers of 2.5 ml each. The exposed area was 0.1 cm^2. Vigorous stirring was maintained with magnetic bars rotating on the flat floor of the chamber and by bubbling moistened compressed air with 5% CO_2. The electrical resistance across the disk was monitored by passing 20 µA of current via two chlorided silver wires placed at 2 cm from the monolayer and recording the voltage deflection with a high input impedance voltmeter ($10^{10}\,\Omega$) connected to a couple of plated silver electrodes placed very close (<0.3 mm) to the disk. The electrical resistance of a disk without MDCK monolayer was measured beforehand with the same setup, and substracted from the values obtained with the complete preparation. Tracer sodium (5 µCi of ^{22}Na from New England Nuclear Corp., Cambridge, Mass.) was added to one of the chambers and 5–10 samples of 0.5 ml were taken every 5 min from the opposite side. The volume was replaced with fresh Ringer. At the beginning and at the end of the sampling period, 100 µl of the outer solution was taken and diluted for counting. All determinations were made in MEM without serum, at 37 °C. During the experimental period both bathing solutions behave as infinite reservoirs.

Na Fluxes Across the Plasma Membranes of MDCK Cells

a) Washout. The Petri dishes with the confluent monolayers were twice washed with Ringer solution containing (mM): 118 NaCl, 22 $NaHCO_3$, 1.8 $CaCl_2$, 1.0 $MgCl_2$, 5.0 glucose, pH 7.4. They were then incubated for 30 min in the same solution. This solution was then replaced by 1.0 ml of fresh Ringer containing 1 µCi of ^{22}Na and left in the incubator at 37 °C for 2.5 hr. After this loading period, monolayers were quickly washed two times with cold $MgCl_2$ solution and left in contact with this solution at 4 °C for 2 min. Studies by J. Ehrenfeld and M. Cereijido (*submitted for publication*) have shown that during this wash 70–80% of the extracellular sodium is eliminated and the cellular compartment does not change. In order to avoid contamination with the remaining 20–30% of extracellular ^{22}Na, the first period (1 min) of the washout was also discarded. The washout of ^{22}Na from cells was then followed by incubation of monolayers with 1.0 ml of Ringer at 37 °C. After 1 min the Ringer was collected for ^{22}Na counting and the Petri dish refilled with fresh Ringer. The procedure was repeated 4–5 times. The composition of the several Ringers used for the washout is given in Results. At the end of the sampling period, 1.0 ml of 1.0 N H_2NO_3 was added and left 1 hr at room temperature. This fluid was then analyzed for total and tracer sodium using a Varian flame photometer (Unicam SP90, England) and a Nuclear Chicago Auto Gamma Counter (Chicago, Ill.).

b) Uptake. The monolayers were washed as above, and incubated with the same Ringer solution containing 10^{-4} M ouabain for 2 hr at 37 °C. This solution was then replaced by a fresh one containing 1.0 µCi of ^{22}Na and left for 3.0 min. This time was chosen on the basis of preliminary experiments which indicated that saturation was reached in 2–3 hr and that during the 3.0-min period the uptake curve remained linear. The loading solution was then discarded, and the monolayer was quickly washed with cold 0.1 M $MgCl_2$ and left in contact with this solution for 2.0 min at 4 °C. This washing procedure does not modify the pool of radioactive sodium, but reduces the amount of tracer trapped in the extracellular space (*unpublished results*). At the end of this period the $MgCl_2$ solution was removed, and ^{22}Na was extracted for counting, as in the case of the washout.

^{3}H-Ouabain Binding

Disks containing monolayers were mounted as flat sheets between two chambers. Their position was horizontal and the side to be labeled faced down. The volumes of upper and lower chambers were 0.5 and 3.0 ml, respectively. The lower one was vigorously stirred by a magnetic bar. Labeled ouabain (New England Nuclear Corp., Cambridge, Mass., 19 mCi/mmol) was added to the lower chamber. The concentrations of labeled and unlabeled ouabain were 5×10^{-7}M and 10^{-4} M, respectively. Incubation lasted 2 hr at 36.5 °C. The upper solution was changed every 15 min to keep it clean of ^{3}H-ouabain, as it was observed that ouabain has a small but detectable flux across the monolayers. At the end of

the incubation period the disk, still in position, was rinsed with 0.85% saline solution at 1.0 °C, and a sample of 0.24 cm^2 of the exposed area was obtained with a cork borer. This sample was washed with 200 ml of cold saline for 10 min. The sample was put in 0.5 ml of 0.6 N NCS Tissue Solubilizer (Amersham Corp., Buckinghamshire, England) and left overnight in a Wrist Action Shaker (Burrell Corp., Pittsburgh, Pa.). The β emission was counted using PPO and POPOP mixture dissolved in toluene in a Packard liquid scintillation counter. ^3H activity was also measured in the bathing media.

Freeze Fracture

Confluent monolayers of MDCK cells grown on collagen-coated nylon disks were fixed for 30 min with 2.5% glutaraldehyde in 0.1 M cacodylate buffer, pH 7.3, at room temperature. After fixation, the monolayers were washed two times with 0.1 M cacodylate buffer, and separated from the nylon mesh by gently scraping the surface with a glass coverslip under a dissecting microscope. The monolayer easily separated from the nylon disk with the collagen layer attached. To facilitate separation, nylon disks were covered with a collagen coat thicker than that used for electrophysiological measurements. The fixed monolayers were gradually impregnated with increasing concentrations of glycerol in cacodylate buffer during a 30-min period, up to a concentration of 20% glycerol, where they were left for 30 min.

Fixed, glycerol-impregnated MDCK monolayers were rapidly frozen in the liquid phase of partially solidified Freon 22, cooled by liquid nitrogen, and stored in liquid nitrogen for 1–3 days. Freeze-fracture was carried out at −120 °C in a Balzers 300 (Liechtenstein) apparatus equipped with a turbomolecular pump.

Replicas were produced by evaporation from a carbon-platinum source. The specimens were shadowed at 2×10^{-6} mm Hg within 2–4 sec of fracturing and the knife positioned under conditions that minimize contamination. After cleaning in sodium hypochlorite, replicas were washed with distilled water, mounted on Formvar-coated grids, and observed with a Zeiss EM 10 (Oberkochen, Germany) electron microscope. Micrographs are mounted with the shadow direction from bottom to top.

Quantitation of the number of intramembrane particles on *P* and *E* faces (Branton *et al.*, 1975) of plasma membranes of MDCK cells was carried out on positive prints of electron micrographs of uncontaminated flat regions where the shadow angle was uniform, using a final magnification of ×120,000. A Zeiss TGZ 13 Particle Counter (Oberkochen, Germany) was used to estimate the number of IMP/μm^2. For measurement purposes we only used regions of fractured plasma membrane with a total surface of 0.5 or 1 μm^2. Positive identification of the three membrane regions studied, apical, lateral, and basal, was achieved taking into account: (i) the presence of fractured microvilli in the case of the apical surface; (ii) desmosomes, tight junctions, and lack of microvilli at lateral regions; and (iii) lack of junctional complexes, abscence of microvilli, and presence of pinocytotic vesicles in basal regions. Estimations of the IMP numerical densities at the lateral aspect of plasma membranes were carried out only in regions where IMP showed a uniform distribution, thus avoiding desmosomes. Further aspects on the technique have been published in detail elsewhere (Martínez-Palomo, Chávez & González-Robles, 1978).

The ultrastructural study of thin sections of MDCK cells was carried out in confluent monolayers grown on Petri plastic dishes, fixed for 30 min with 2.5% glutaraldehyde in 0.1 M cacodylate buffer, pH 7.3, postfixed during 10 min with 1% osmium tetroxide in cacodylate buffer, dehydrated in increasing concentrations of ethanol, and separated from the plastic substrate by a brief incubation in propylene oxide. After detachment of the complete monolayer, cells were transferred to a large volume of propylene oxide and subsequently embedded in Epon 812. Thin sections perpendicular to the surface of the monolayer were cut with diamond knives and examined with the electron microscope, after staining with lead and uranyl salt solutions.

Preparation of Antibodies

Tubulin was obtained from bovine brain by polymerization cycles (Shelanski, Gaskin & Cantor, 1973) and further purified by chromatography in DEAE-cellulose (Bryan & Wilson, 1971). Actin was purified from rabbit skeletal muscle (Spudich & Watt, 1971). Both proteins were checked for purity in 8-M urea-sodium dodecyl sulfate

Table 1. Unidirectional fluxes of sodium across epithelial membranes

Preparation	Animal	Influx	Efflux	Net	References
		($\mu mol\ hr^{-1}\ cm^{-2}$)			
Proximal tubule, kidney[a]	*Necturus*	961	738	223	Oken *et al.* (1963)
MDCK monolayers[a]		*22.8*	*20.5*	*2.6*	*This work*
MDCK monolayers[a]		17.8	—	—	Barker & Simmons (1978)
Ileum mucosa[a]	Rabbit	14.3	10.5	3.7	Field *et al.* (1971)
Ileum	Rat	12.0	8.5	3.5	Curran *et al.* (1957)
Ileum	Rabbit	9.5	6.7	2.8	Schultz & Zalusky (1963)
Colon	Rat	8.9	6.7	2.2	Curran & Schultz (1968)
Ileum	Dog	8.6	15.9	—	Curran & Solomon (1957)
Gallbladder	Fish	8.4	—	—	Diamond (1962)
Cacum	Guinea pig	7.8	5.1	2.7	Ussing & Andersen (1955)
Colon	Rat	5.3	3.2	2.1	Curran & Schwartz (1960)
Ileum	Rat	4.7	2.1	2.6	Curran (1960)
Skin	Frog (*Leptodactylus ocellatus*)	3.0	0.19	2.8	Zadunaisky *et al.* (1963)
Skin	Frog (*Rana pipiens*)	1.05	0.16	0.89	Cruz & Biber (1976)
Gastric mucosa[a]	Frog	0.49	0.49	—	Hogben (1955)

[a] These preparations consist of pure epithelia. The rest of the values correspond to fluxes across the whole wall of the organ.

polyacrylamide gel electrophoresis. Antibodies were induced by injection of the denatured proteins into rabbits using Freund's adjuvant. The titer of the antibodies produced was verified by immunoprecipitation of the ^{125}Iodine-labeled antigens. Monospecific antibodies were obtained by adsorption of the immune-gamma globulins to Sepharose 4B (Pharmacia, Sweden) columns, to which purified tubulin or actin were cross-linked.

Immunofluorescence Assays

Cells were grown to confluence on glass coverslips. Cytoskeleton, where microtubules were preserved, were prepared by lysing unfixed cells with 0.5% Triton X-100 in a PIPES (piperazine-N, N'-bis (2-ethane sulfonic acid)) sodium salt buffer containing polyethylene glycol 6000 as described by Osborn and Weber (1977). Treated cells were then washed with the buffer without detergent, fixed 10 min with cold methanol, and postfixed with 2% formaldehyde. For the preservation of cytoskeletal microfilaments, unfixed cells were lysed with 0.5% Triton X-100 in Tris-glucose, $MgCl_2$, $CaCl_2$, pH 7.4 buffer (TGMC) as indicated by Brown, Levinson and Spudich (1976). After this treatment, cells were washed and fixed as described above. Antibodies were used at concentrations of 100 µg/ml. The second antibody, fluorescein-labeled goat-anti-rabbit IgGs, was purchased from Miles Laboratories (Elkhart, Ind.) and used at 1:10 dilution. The coverslips were mounted on glass slides with phosphate buffer solution in glycerol. The microscope used was a Standard 18 Zeiss (Oberkochen, Germany) with epifluorescence and photographic attachments.

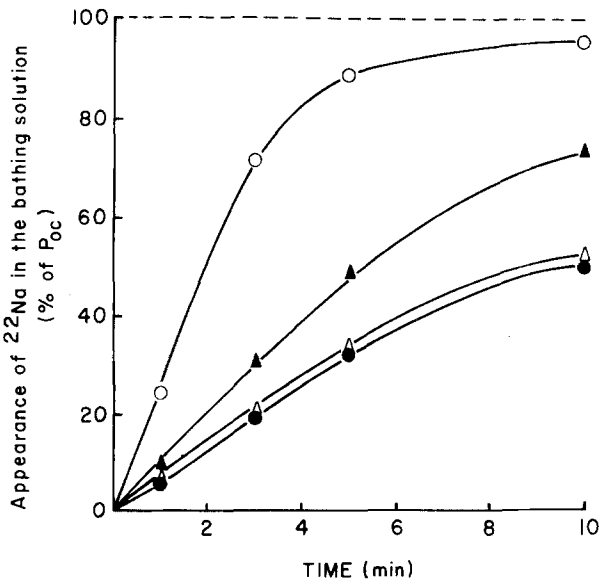

Results

Na-Fluxes Across MDCK Monolayers

Unidirectional sodium fluxes were calculated by measuring 56 periods of influx (apical-to-basolateral) and 73 periods of outflux (basolateral-to-apical) of 5 min each in 16 disks. Influxes were 22.9 ± 0.5 and outfluxes were 20.3 ± 0.4 µmol hr^{-1} cm^{-2}. These values are similar to the one found by Barker and Simmons (1978) for the influx of Na (17.8 µmol hr^{-1} cm^{-2}) for MDCK cells of the same number of passages as the ones used in the present work. These values are much lower than 961 and 738 µmol hr^{-1} cm^{-2} measured by Oken *et al.* (1963) in the proximal kidney tubule of *Necturus* (Table 1) and somewhat higher than those measured in other leaky epithelia. The difference of 2.6 µmol hr^{-1} cm^{-2} between the two fluxes is similar to that observed in most epithelia. Large unidirectional fluxes, assumed to cross through paracellular routes, are characteristic of leaky epithelia. It is interesting to note that, while unidirectional

Fig. 1. ^{22}Na washout as a function of time. In three groups of monolayers the cells were preincubated with 10^{-4} M ouabain for 2.5 hr. The washout was studied in sucrose Ringer (●) containing (mM): 10 Tris at pH 7.4; 1.8 $CaCl_2$; 1.0 $MgCl_2$; and 5 glucose. Sucrose was added to adjust the osmolarity to 300 mosM. A second group was washed with sucrose Ringer with 10 mM KCl (△) and a third one was washed with a Ringer where sucrose was replaced on an osmolar basis by NaCl (▲). A fourth group of monolayers was not preincubated with ouabain (○) and was washed with sucrose Ringer containing 10 mM KCl. Each point is the average of 4 monolayers and the SE is less than 5%

Table 2. Washout of sodium of MDCK monolayers

		Washout medium		
		Ringer sucrose	Ringer sucrose with 10 mM K	Ringer Na
Preincubated without K, and ouabain (10^{-4} M)	k_{cm}	0.071 ± 0.004	0.079 ± 0.003	0.141 ± 0.002
	J_{cm}	0.072 ± 0.003	0.090 ± 0.003	0.397 ± 0.018
Preincubated without K	k_{cm}		0.506 ± 0.017	
	J_{cm}		0.450 ± 0.032	

Ringer sucrose contains (mM): 1.0 $MgCl_2$, 1.8 $CaCl_2$, 5.0 glucose, 10 Tris HCl, pH 7.4; sucrose was added to adjust the osmolarity to 300 mosM. Ringer sodium contains the same basic components, but sucrose is replaced by 140 mM Na. The rate constant (k_{cm}) for sodium extrusion from the cells to the medium is expressed as min^{-1} and fluxes (J_{cm}) as µmol hr^{-1} cm^{-2}.

fluxes are very large and different in the several epithelia listed in Table 1, the net flux is analogous in all of them. This suggests that the differences between epithelia are mainly due to the permeability of the paracellular route. Although this net flux is similar to those observed in natural epithelia, it is calculated as the difference between two large unidirectional fluxes and, therefore, subject to a considerable experimental error.

Na-Fluxes Across the Plasma Membrane of MDCK Cells

a) Sodium Efflux. Figure 1 and Table 2 show the efflux of Na from cells that, during the loading with tracer Na, were preincubated at 37 °C in a Ringer without K and with ouabain added. The Na pool in the cells of resting monolayers incubated in CMEM or in regular Na-Ringer is too small and washes its Na tracer too fast to be amenable for study with the methods available and with a small error. Therefore, we increased the Na pool by removing K or adding ouabain to stop the Na pump during the preincubation (Smith & Rozengurt, 1978; M.J. Rindler, *personal communication*). The results shown below indicate that the increase of the Na pool permits the detection of several mechanisms that the MDCK cell uses to extrude Na.

The unidirectional flux from the cells to the bathing medium (J_{cm}) was calculated as follows:

$$J_{cm} = k_{cm} S_c \tag{1}$$

where k_{cm} is the rate constant for the washout of ^{22}Na, and S_c is the Na pool of the cells. S_c was taken as the Na content at the beginning of the washout period. This assumption is made for the sake of comparison of the different experimental conditions listed in Table 2, which were processed in exactly the same manner. It should be pointed out that this calculation affords a maximum estimate of J_{cm}, as S_c is maximal at the beginning of the washing period.

The upper two lines of Table 2 correspond to monolayers where, in order to study passive mechanisms, the pump was blocked both with ouabain and by removing potassium. When these monolayers were washed in sucrose Ringer, which is a very restricted medium, i.e., one in which most mechanisms would be impaired, we measured a rate constant (k_{cm}, the subindex stands for cell-to-medium) of 0.071 min^{-7}, and a flux of 0.072 μmol hr^{-1} cm^{-2}. The addition of K to the bathing solution (second column) does not modify significantly the values of these parameters, because the pumps were inhibited with ouabain. The addition of Na (third column) accelerates the exit of Na from the cells, as it increases the values of the rate constant and the flux. This enhancement of the extrusion of Na by the presence of the same ion on the contralateral side indicates that one of the mechanisms of Na translocation in MDCK cells is an exchange diffusion process.

While the effect of ouabain is very poorly reversed, the restoration of K activates the pump instantaneously. Therefore, in order to study the presence of a pump, instead of using ouabain during the preincubation, we inhibited the pump by removing K only. The restoration of K produces a significant increase of the efflux as compared with the situation listed in the upper part of the same column where the pumps are blocked by ouabain (0.450 *vs.* 0.090 μmol hr^{-1} cm^{-2}.

Effect of Amiloride

Amiloride(2,5-diamino-6-chloropyrazinoylguanidine; Merck, Sharp & Dohme; West Point, Pa.) is a known inhibitor of Na penetration across the apical border of epithelial cells (Eigler & Crabbe, 1969). At high concentrations it also inhibits Na uptake in MDCK monolayers (Rindler & Saier, 1978). This observation is here confirmed. Amiloride, 10^{-3} M, lowers the influx from 0.129 ± 0.009 to 0.073 ± 0.009 ($n=4$) μmol hr^{-1} cm^{-2}. This difference, 0.056 μmol hr^{-1} cm^{-2} is highly significant ($P<0.001$). This is a further similarity of MDCK monolayers with natural transporting epithelia. It may be noticed that the value of the influx in this set of monolayers is lower than the efflux reported in Table 2 (third column). As mentioned above, the use of the initial value of S_c in the calculation of the outflux affords a maximum value of J_{cm}. Fluxes measured in a given set of membranes had very similar values, as shown by their small standard deviation. However, monolayers prepared on different days may exhibit a considerable

Table 3. Unilateral labeling of MDCK monolayers with ^{3}H-ouabain

Group	^{3}H-ouabain added to[a]	Nonlabeled ouabain[b]	10^{11} molecules bound per cm^2
1	Basolateral	Absent	29.7 ± 1.8 (5)
2	Basolateral	Added	2.5 ± 0.8 (5)
3	Apical	Absent	1.8 ± 0.4 (5)
4	Apical	Added	0.4 ± 0.1 (5)

[a] 5×10^{-7} M of ^{3}H-ouabain.
[b] 10^{-4} M ouabain.

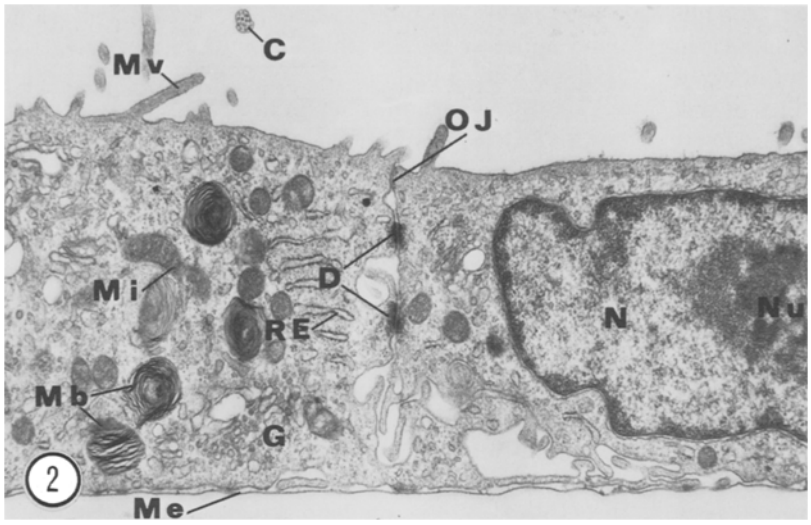

2. Cross section of MDCK monolayer at
egion of intercellular contact between two
. In the lumenal region a few microvilli
) are present, as well as a transverse section
cilium (*C*). The lateral side of the plasma
ıbrane is characterized by short occluding
tion (*OJ*), two desmosomes (*D*), and
ular interdigitations. The basal aspect rests
ı a thin carpet of microexudate (*Me*),
chondria (*Mi*), components of the Golgi
ıratus (*G*), and rough endoplasmic
ulum (*RE*), and multilamellar bodies (*Mb*)
ocated laterally to the nucleus (*N*) that
vs a prominent nucleolus (*Nu*). × 7,000

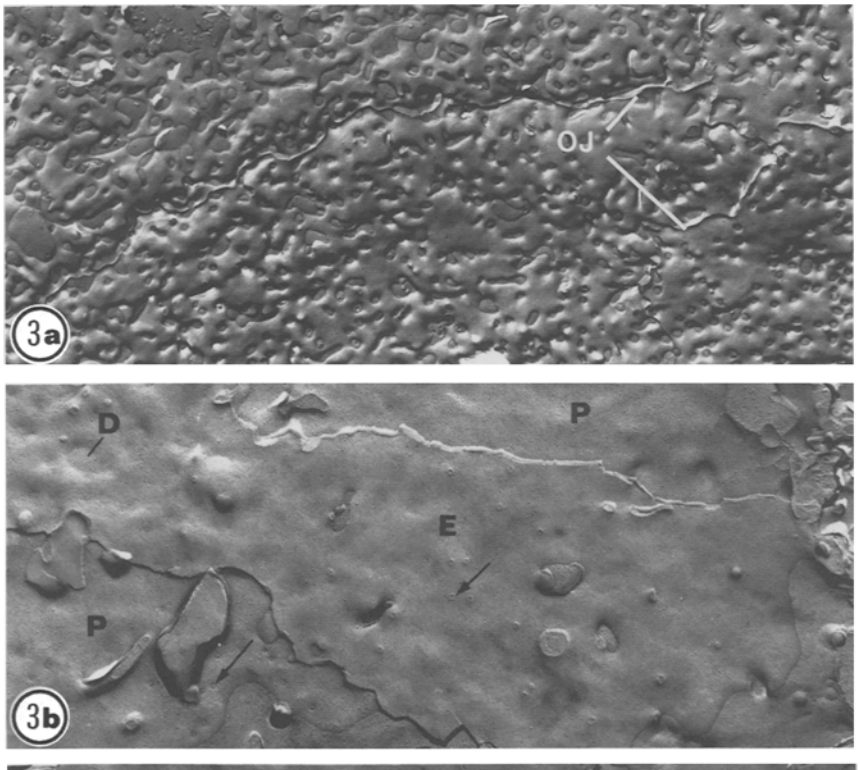

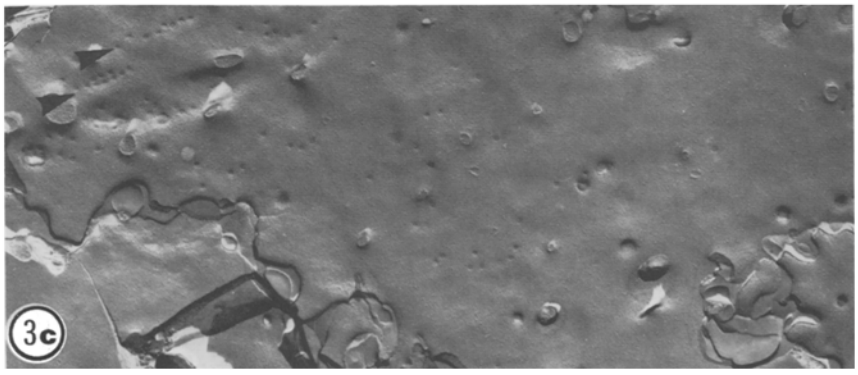

Fig. 3. Low magnification views of different plasma membrane regions of MDCK cells seen in freeze-fracture replicas. (*a*): Portions of the *E* face of the lumen region of four cells. The membranes show abundant fractured microvilli and the cellular outlines limited by the occluding junctions (*OJ*). × 10,000. (*b*): The lateral aspect of the plasma membrane with both *E* and *P* fracture faces (*A*, *P*). Desmosomes (arrowheads) and scarse pinocytotic vesicles (arrows) are present. × 13,000. (*c*): Basal aspect of the plasma membrane characterized by abundant pinocytotic vesicles, some of which are aligned in rows (arrowheads). × 13,000

variability. It is known that factors like the schedule in the change of medium, variations in the concentration of the serum, and length of time in confluence may vary the ionic content and the ionic flux of cultured cells (Rozengurt & Heppel, 1975; Tupper, Zorgniotti & Mills, 1977; Ehrenfeld, *unpublished results*).

Binding of ^3H Ouabain

Disks were divided into four groups (Table 3): *group 1:* basolateral side in contact with ^{3}H-ouabain. *Group 2:* basolateral side in contact with ^{3}H-ouabain, plus nonlabeled ouabain at a 200-times higher concentration. The addition of nonlabeled ouabain was

Table 4. Morphological polarization of MDCK cells as seen in freeze-fracture replicas

Region	General morphology	Numerical densities of IMP (IMP/μm^2 + SE)	
		P face	*E* face
Apical	Microvilli	599 ± 43	388 ± 30
Lateral	Cell junctions: desmosomes, occluding junctions Cellular interdigitations Sparse micropinocytotic vesicles	1,365 ± 105	286 ± 14
Basal	Lack of microvilli and cellular junctions Abundant micropinocytotic vesicles aligned in rows	1,468 ± 40	462 ± 38

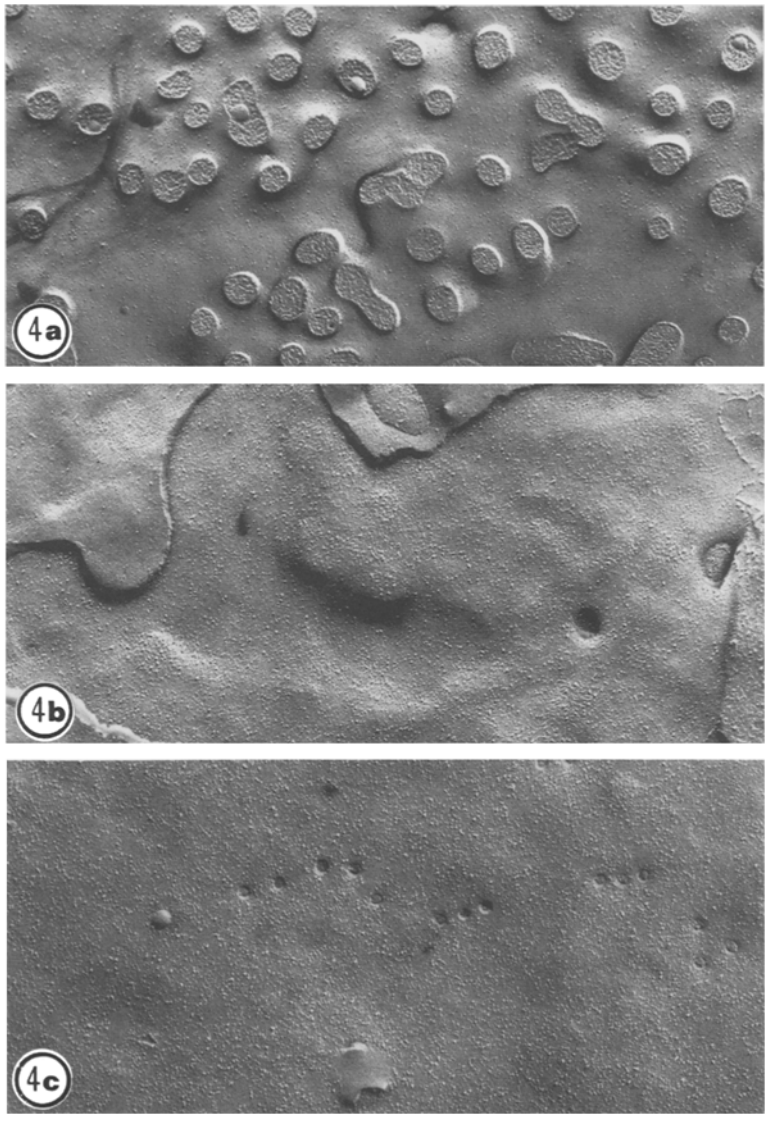

Fig. 4. Higher magnification of freeze-fracture replicas of different regions of MDCK plasma membranes. (*a*): Lumenal region, *P* face. ×35,000. (*b*): Lateral region, *P* face. ×35,000. (*c*): Basal region, *P* face. ×25,000

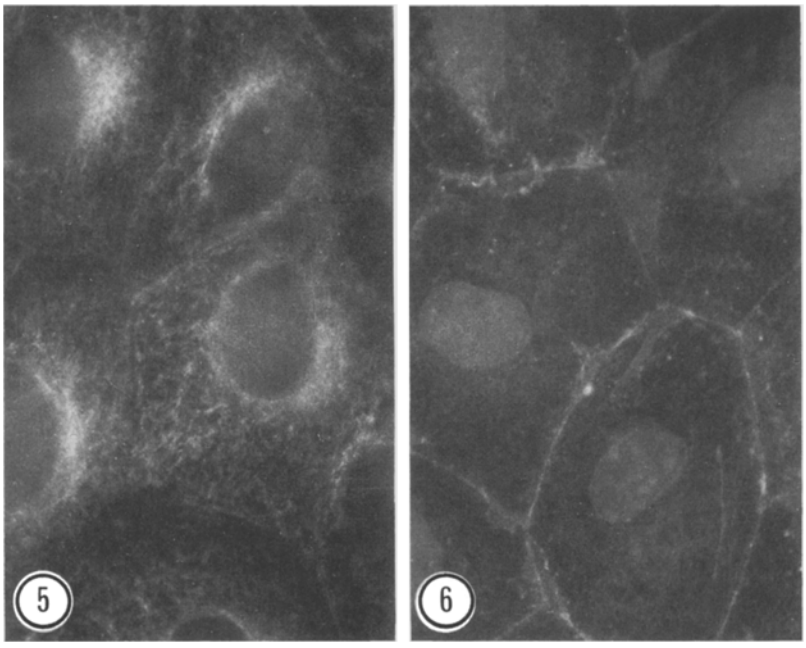

Fig. 5. Microtubular pattern of MDCK monolayers. Cells were treated for 2 min with stabilization buffer containing 0.5% Triton X-100. Microtubules can be followed from the perinuclear region to the periphery of the cells and extending into the cell processes where they follow the contour of the cell. × 1,300

Fig. 6. Actin-microfilament pattern in MDCK monolayers. Cells were treated with TGMC buffer containing 0.5% Triton X-100 for 5 min. Microfilaments are visualized as a fine network extending to the edges of the cell and forming a continuous ring under the lateral surface. × 1,300

intended to compete, displace, and dilute ^{3}H-ouabain from all specific binding sites and confine it to nonspecific attachment and unwashed interstices. It was assumed that labeling in the presence of cold ouabain (groups *2* and *4*) measured nonspecific binding and, therefore, the difference between groups *1* and *2* was taken to represent the labeling of specific sites (Dunham & Hoffman, 1971; Sachs, 1977; Joiner & Lauf, 1978). *Groups 3 and 4* are analogous to groups 1 and 2, but for the apical side.

The basolateral side has 27.2×10^{11} Na-pumping sites/cm^2 (i.e., 29.7 minus 2.5), and the apical side has 1.4×10^{11} sites. This shows that the distribution of Na-pumps in MDCK cells is asymmetric, a feature that stresses further the analogy of this cultured monolayer with natural transporting epithelia.

Thin-Section Electron Microscopy

The morphological polarization of MDCK cell monolayers studied in cross section is evidenced by the presence of microvilli at the lumenal side of the cell, and by the focal obliteration induced by occluding junctions at lateral intercellular spaces. Desmosomes are commonly found at the lateral sides of adjacent plasma membranes; occasionally cilia may be present at the apical border (Fig. 2). A microexudate layer 8–10 nm thick is constantly found attached to the basal side of the monolayer. The polarization of cytoplasmic components is mainly reflected in the basal location of nuclei and the lateral concentration of most organelles, such as mitochondria, rough endoplasmic reticulum and Golgi apparatus components, lipid vesicles, and multilamellar bodies.

Freeze-Fracture Electron Microscopy

The morphological polarization of the MDCK cell plasma membrane is clearly evidenced in replicas of freeze-fractured monolayers examined with the electron microscope. The fractured membranes show three structurally distinct domains: an apical region characterized by a uniform and abundant population of microvilli fractured at their base (Fig. 3*a*); the lateral region represented by smooth membrane faces with broad interdigitations (Fig. 3*b*), and the basal aspect of the plasma membrane depicted as flat membrane fracture faces with abundant pinocytotic vesicle's (Fig. 3*c*).

Replicas usually contain extensive areas of fractured apical and basal membrane regions, whereas lateral regions fracture less extensively. Positive identification of lateral and basal membrane regions can only be achieved in replicas where the fractured plasma membranes are framed within the general morphology of the cell.

The distribution of intramembrane particles (IMPs) is different in the three above-mentioned regions of the plasma membrane. The numerical densities of IMPs, their topographical distribution, and

the diameter and shape of IMP population varies from one region to another. In apical and basal regions, IMPs show a random distribution as judged by visual examination. In contrast, a readily recognizable pattern of IMPs distribution is found in the lateral aspects, where membrane particles form occluding junctions at the apico-lateral side (Misfeldt *et al.*, 1976; Cereijido *et al.*, 1978). Desmosomes appear at various levels of lateral membranes as slightly raised oval areas on *P* faces and complementary depressions on *E* faces, where fibrillar and granular IMPs accumulate. Gap junctions (conmunicating junctions) were never found in replicas of MDCK cells.

Pinocytotic vesicles appear mostly on the basal aspect of the plasma membrane. The vesicles frequently align following one or two parallel rows. They are not restricted to the basal region, since occasionally vesicles may be found at the lateral sides (Fig. 3*c*).

In addition to the gross morphological differences that indicate polarization of the plasma membrane of MDCK cells, i.e., microvilli in apical regions, cell junctions in the lateral aspect, and pinocytotic vesicles mostly in the basal side, another indication of membrane polarity is the difference in the numerical densities of IMPs.

As shown in Table 4, *P* and *E* faces of apical regions of MDCK cell plasma membranes show a sparse population of IMPs: 599 ± 43 for *P* faces and 388 ± 30 for *E* faces. IMPs tend to be heterogeneous in size and diameter on *E* faces, in comparison to complementary *P* faces (Fig. 4*a*). Lateral membranes (Fig. 4*b*) show a much higher density of IMPs on *P* faces: $1{,}365 \pm 105$. *E* faces at lateral membranes average 286 ± 14. The basal region also has a high density of IMPs on *P* faces: $1{,}468 \pm 90$ (Fig. 4*c*). *E* faces at basal membranes have a mean of 462 ± 38. The sparsity of IMPs at *P* faces of the luminal side and the dense population of IMPs on *P* faces of the lateral region are sharply delimited by the occluding junctions, which appear to act as a transmembrane barrier to define two membranes domains, each provided with different populations of IMPs. As in the apical region, IMPs on *E* faces of lateral and basal zones constitute a more heterogeneous population in terms of their size and diameter.

Cytoskeleton

As mentioned in the introduction, maintenance of the asymmetry of membrane components is generally associated with the cytoskeleton. Accordingly, we used immunofluorescent antibodies to study the pattern of distribution of microtubules and microfilaments and their association with membrane components.

Microtubules, as visualized with anti-tubulin antibody staining are concentrated around the nucleus and from here extend radially towards the plasma membrane where they become extremely fine. Fibers are also seen parallel to the plasma membrane following the outline of the cell and extend into the cellular processes (Fig. 5). The pattern observed in the lysed cells (cytoskeletons) is the same as that seen in the intact cells, except that in the cytoskeletons the fibers are more clearly delineated and their total extension can be determined.

Microfilaments, identified with anti-actin antibody, also run from the perinuclear region, forming an extensive network that reaches the periphery of the cell as very fine threads. The most striking feature is the continuous ring formed by microfilaments at the lateral region of the cell membranes (Fig. 6) where cells attach to each other. On the other hand, actin cables as those seen in fibroblastic cells (Osborn *et al.*, 1978) were not found. Since occluding junctions are considered as barriers separating apical from basolateral components and, moreover, the microfilaments in the cytoskeleton participate in the regulation of the permeability and reassembly of the junctions (Meza *et al.*, 1978), it may be inferred that they play a role in the maintenance of the asymmetry of the plasma membrane.

Discussion

The experimental observations here reported tend to support the notion that the plasma membrane of MDCK monolayers in culture shows structural and functional polarity, comparable to those of natural epithelia. Thus, MDCK cells exhibit the following characteristics: (i) they have a net transepithelial transport of Na; (ii) the penetration of Na into the cells depends on an amiloride-sensitive channel; (iii) the net transport of Na from the apical to the basolateral side agrees with the asymmetric labeling of the Na pumps with ^{3}H-ouabain; (iv) the functional asymmetry is accompanied by an asymmetric distribution of IMPs in freeze-fracture replicas of plasma membranes; (v) they show morphological polarization evidenced by the asymmetric location of microvilli, occluding junctions, and pinocytotic vesicles; and (vi) the close apposition of adjacent cells and the formation of occluding junctions, which maintain the polarity of the plasma membrane, are related to the formation of specific patterns of cytoskeletal components.

The asymmetry of the MDCK plasma membranes

Table 5. Sodium pumping sites as estimated by ^{3}H-ouabain binding

Preparation	Animal	Pumps	Pumped ions[a]	References
		(molecules · 10^8/cm^2)	(ions/site · sec)	
MDCK monolayer		27.190 Ba[b]	22–161	This work
Choroid plexus	*Rana*	10.000 Ap[c]		Quinton *et al.* (1973)
MDCK monolayer		1.140 Ap		This work
Nerve	Rabbit	750	22	Landowne & Ritchie (1970)
Smooth muscle	Guinea pig	250	22	Brading & Widdicombe (1974)
Adipocytes		66		Clausen & Hausen (1974)
Erythrocytes	Human	1	175	Ellory & Keynes (1969)
Erythrocytes	Human	1	150	Hoffman (1969)
		(10^5 molecules/cell)		
Giraldi cells (heart)	Human	497		Baker & Willis (1972)
HeLa cells	Human	266		Baker & Willis (1972)
Kidney cells	Guinea pig	182		Baker & Willis (1972)
MDCK monolayer		92 (Ba)		This work
		(10^{11} molecules/mg wet wt)		
Salt gland	Bird	883.0		Ernst & Mills (1977)
MDCK monolayers		46.1		This work
Brain	Guinea pig	14.0	217	Baker & Willis (1972)
Kidney cortex	Guinea pig	14.0		Baker & Willis (1972)
Kidney	Guinea pig	10.3		Baker & Willis (1972)
Nerve	Squid	3.5[d]		Baker & Willis (1972)
Skin	*R. Catesbiana*	2.9 Ap		Mills *et al.* (1977)
HeLa cells	Human	2.7	92	Baker & Willis (1972)
Liver	Guinea pig	1.6		Baker & Willis (1972)
Nerve	Crab	1.3		Baker & Willis (1972)
Urinary bladder	Frog	0.9 Ap		Mills & Ernst (1975)
Skeletal muscle	Frog	0.7	3.3	Grinstein & Erlij (1974)
Choroid plexus	Frog	15.0 Ba		Quinton *et al.* (1973)
Heart	Guinea pig	0.1	2275	Dutta & Marks (1969)
Erythrocyte	Human	0.025	83	Baker & Willis (1972)
Urinary bladder	*Rana*	0.024 Ap		Mills & Ernst (1975)
Erythrocyte	Guinea pig	0.019	140	Baker & Willis (1972)

[a] Assuming a molecule of ouabain bound corresponds to a pump.
[b] Ba: basolateral.
[c] Ap: apical.
[d] ^{3}H-ouabain binding was measured at 18–20 °C. In the other preparations it was measured at 36.5 °C.

is not absolute, as the lumenal side is labeled to some extent with ^{3}H-ouabain, and exhibits a sparse population of IMPs. With the exception of the choroid plexus (Quinton, Wright & Tormey, 1973), we know of no other epithelium with Na pumps on the apical side. This would indicate that apical labeling of MDCK monolayers might be due to contamination of the nonradioactive bathing solution with ^{3}H-ouabain leaking from the lower to the upper chamber. However, the specific labeling of the apical sites may also represent an incomplete asymmetry of the distribution of Na pumps, as found in cells of the proximal segments of renal convoluted tubules (Kyte, 1976). Yet, data in Table 3 show that the distribution of pumps is asymmetric enough to account for the net inward Na flux. This result is in keeping with the following facts: (i) MDCK monolayers cultured on nonpermeable supports produce blisters attributed to the accumulation of water (Leighton *et al.*, 1969; Rabito *et al.*, 1978); (ii) transport of water between isotonic media is not a primary phenomenon, but arises from coupling to solute transport; and (iii) blister formation in MDCK monolayers is inhibited by ouabain (Abaza, Leighton & Schultz, 1974).

Table 5 compares the values obtained in MDCK monolayers with those of natural epithelia. The upper group shows the number of Na pump sites per square centimeter. It is obvious that epithelia whose cells need pumps not only to keep their own Na balance, but to transport Na across, have a greater number

of pumps that single cells. However, while the area of single cells listed in Table 5 corresponds to the area of their plasma membrane, in an epithelium the area of plasma membrane per square centimeter of tissue is much higher. Therefore we converted the results to pumps per cell (Table 5, second group). To obtain the necessary data, we took photographs of our preparation, measured the area of the windows (1.42×10^{-4} cm^2) and the number of cells in each window (41.8 ± 0.7, 20 windows), which results in 2.95×10^5 MDCK cells per cm^2. This means that the MDCK cells have 92×10^5 Na pump sites on the basolateral side and 5×10^5 on the apical one. Although this procedure has the inconvenience of assuming that the cells of the different tissues listed in Table 5 have equal size, it shows that the data of MDCK monolayers are comparable to those of natural preparations. To compare our results with those available in the literature which are expressed in sites per mg of tissue, we converted our results to 46.0×10^{11} sites/mg for the basolateral side and 2.4×10^{11} for the apical one. Again, the population of Na pump sites in MDCK monolayers is similar to those in natural tissues.

When values of Na fluxes were also available, we computed the number of Na ions pumped per site and per second (Table 5, third row). If the 2.6 μmol hr^{-1} cm^{-2} of net flux observed is attributed to Na pumps, the 27.2×10^{11} sites per cm^2 on the basolateral side will pump 161 Na ions per sec. The same calculation, performed with the Na flux obtained in the washout (Table 2) gives 22 Na ions per each site and per sec. This value of ^{22}Na ions may be more reliable because, as explained above, the evaluation of the active flux is more accurate than the net flux calculated as a difference between two large unidirectional fluxes. These figures may not depend on the fact that the pump belongs to an epithelioid cell, but to the intrinsic mechanism of the pump, which might be common to all kind of cells. The 22 to 161 ions per sec pumped by a site in the MDCK cells, compares with the 140 pumped by a site in red blood cells, and the 217 translocated by a pump in the brain.

Previous studies on MDCK monolayers have centered on the role of the passive paracellular pathway as a transcellular route for epithelial fluxes limited by the occluding junctions (Misfeldt *et al.*, 1976; Cereijido *et al.*, 1978). Other properties such as vectorial transport of ions and small molecules across the epithelial cells require that the lumenal and the basolateral side of plasma membrane to be endowed with different specialized components, as shown in the present study. In recent years, freeze-fracture electron microscopy has revealed the structural polarity of epithelial plasma membranes, mainly as differences in the population density of IMPs between *P* faces of apical and basolateral membrane regions. The *P* face of the lumenal portion of the plasma membranes, which is surrounded by the occluding junction, is characterized by a low density of IMPs relative to the *P* face of the lateral and basal regions in the urinary bladder epithelium of the frog (Chevalier, Bourguet & Hugon, 1974) and of the toad (Wade, DiScala & Karnovsky, 1975), as well as in pancreatic (De Camilli, Peluchetti & Meldolesi, 1974) and parotid guinea pig acinar cells (De Camilli, Peluchetti & Meldolesi, 1976). The segregation of the two distinct membrane domains is maintained by the continuity of occluding junctions, that form a transmembrane barrier which restricts the intermixing of IMPs of the lumenal and the basolateral plasma membrane (Galli *et al.*, 1976; Meldolesi *et al.*, 1978). Similar conclusions have been obtained by studying the redistribution of surface macromolecules in dissociated frog urinary bladder cells by means of ultrastructural autoradiography and cytochemistry (Pisam & Ripoche, 1976). The difference in numerical densities of IMPs in *P* faces of lumenal and basolateral regions of MDCK plasma membranes here reported, strengthen the similarity of this culture system to natural epithelia. Recently, the asymmetry of MDCK monolayers has been further demonstrated by the uneven budding of viruses, either from the free surface or from the basolateral region, according to the type of virus allowed to replicate in MDCK cells (Rodríguez-Boulan & Sabatini, 1978).

One of the basic characteristics of the MDCK monolayers is their ability to form occluding junctions, which help to establish a diffusion barrier and to maintain morphological and functional polarity. An essential requirement in order to form these junctions is that cells make contact with each other and their membrane borders come into apposition. As this requirement is fulfilled, the components of the junctional complexes are positioned and assembled in the apical portion of the lateral side and linked with those in neighboring cells. These processes involve cellular events which are known to be related to the cytoskeleton. Thus, microtubules and microfilaments have been implicated in: topographical distribution of membrane components (Ash & Singer, 1976; Sunqvist & Ehrnst, 1976; Ash *et al.*, 1977), translational mobility of surface components (Gabbiani *et al.*, 1977), membrane transport (Taylor *et al.*, 1976; Frederiksen & Leyssac, 1977), and maintenance of junctional complexes (Bentzel *et al.*, 1976; Meldolesi *et al.*, 1978). Recently the actin microfilaments have also been found to be associated with external membrane protein components (Koch & Smith, 1978;

Moore, Ownby & Carraway, 1978). Although the cytoskeleton has been extensively studied in fibroblastic cells (Brinkley, Fuller & Highfield, 1975, 1976; Weber, Wehland & Herzog, 1976), it has not been characterized in confluent monolayers of epithelial cells. In this study we have visualized, by immunofluorescence, two of the cytoskeletal components, i.e., microtubules and actin-containing microfilaments of MDCK cells. Both components form extensive networks that radiate from the nucleus into the cytoplasm. In the case of microfilaments, a continuous ring is conspicuously present underlying the cell surface in the lateral region where the occluding junctions are also positioned. Disruption of the normal distribution of microtubules and microfilaments with specific drugs (colchicine, cytochalasin B), indicate that their integrity is necessary for the cells to make contact, form the monolayer, and develop transepithelial resistance. Once the junctions are formed, microfilaments, but no microtubules, are the main participants in the maintenance of the structural and functional polarity of the plasma membranes of MDCK cells (Meza *et al.*, 1978).

In conclusion, the results of the present study demonstrate the structural and functional polarity of the plasma membrane of MDCK monolayers in culture. The rapid establishment of this polarity, the homogeneity of the cell population, and the advantages of cell culture render this preparation a suitable model for the study of the differentiation of membrane polarity in epithelia.

This work was supported by Grants 1508 and 1619 from PNCB, 1053 from PRONALSA, CONACYT, Mexico, and AM 26481 from the NIH. J.E. is a recipient of a CONACYT-CNRS fellowship. The authors acknowledge the efficient collaboration of D. Jaén, A. González-Robles, G. Ibarra, A. Lázaro, and M. Sabanero and thank V. Dueñas for excellent secretarial help.

References

Abaza, N.A., Leighton, J., Schultz, S.G. 1974. Effects of ouabain on the function and structure of a cell line (MDCK) derived from canine kidney. *In Vitro* **10**:172

Ash, J.F., Louvard, D., Singer, S.J. 1977. Antibody-induced linkages of plasma membrane protein to intracellular actomyosin containing filaments in cultured fibroblasts. *Proc. Nat. Acad. Sci USA* **74**:5584

Ash, J.F., Singer, S.J. 1976. Concanavalin-A-induced transmembrane linkage of concanavalin A surface receptors to intracellular myosin-containing filaments. *Proc. Nat. Acad. Sci. USA* **73**:4575

Baker, P.F., Willis, J.S. 1972. Binding of the cardiac glycoside ouabain to intact cells. *J. Physiol. (London)* **224**:441

Barker, G., Simmons, N.L. 1978. Dog kidney MDCK cell monolayers can display properties similar to high resistance epithelia. *J. Physiol. (London)* **285**:48*P*

Bentzel, C.J., Hainau, B., Edelman, A., Agnastopoulos, T., Benedetti, E.L. 1976. Effect of plant cytokinins on microfilaments and tight junctions permeability. *Nature (London)* **264**:666

Brading, A.F., Widdicombe, J.H. 1974. An estimate of sodium/potassium pump activity and the number of pump sites in the smooth muscle of the guinea-pig *Taenia coli*, using ^{3}H-ouabain. *J. Physiol. (London)* **238**:235

Branton, D., Bullivant, S., Gilula, N.B., Karnovsky, M.J., Moor, H., Muhlethaler, K., Northcote, D.F., Packer, L., Satir, P., Speth, V., Staehelin, L.A., Steere, R.L., Weinstein, R.S. 1975. Freeze-etching nomenclature. *Science* **190**:54

Brinkley, B.R., Fuller, G.M., Highfield, D.P. 1975. Cytoplasmic microtubules in normal and transformed cells in culture. Analysis by tubulin antibody immunofluorescence. *Proc. Nat. Acad. Sci. USA* **71**:4981

Brinkley, B.R., Fuller, G.M., Highfield, D.P. 1976. Tubulin antibodies as probes for microtubules in dividing and non-dividing mammalian cells. *In:* Cell Motility. A.R. Goldman, T. Pollard, and J. Rosenbaum, editors. p. 435. Cold Spring Harbor Laboratory, Cold Spring Harbor (N.Y.)

Brown, S., Levinson, W., Spudich, J.A. 1976. Cytoskeletal elements of chick embryo fibroblasts revealed by detergent extraction. *J. Supramol. Struc.* **5**:119

Bryan, J., Wilson, L. 1971. Are cytoplasmic microtubules heteropolymers? *Proc. Nat. Acad. Sci. USA* **68**:1762

Cereijido, M., Robbins, E.S., Dolan, W.J., Rotunno, C.A., Sabatini, D.D. 1978. Polarized monolayers formed by epithelial cells on a permeable and translucent support. *J. Cell Biol.* **77**:853

Chevalier, J., Bourguet, J., Hugon, J.S. 1974. Membrane associated particles. Distribution in frog urinary epithelium at rest and after oxytocin treatment. *Cell Tissue Res.* **152**:129

Clausen, T., Hausen, O. 1974. Ouabain binding and Na^+–K^+ transport across cell membranes, and its application to red cell glucose transport. *Biochim. Biophys. Acta* **345**:387

Cruz, L.J., Biber, T.V.L. 1976. Transepithelial transport kinetics and Na entry in frog skin: Effects of novobiocin. *Am. J. Physiol.* **231**:1866

Curran, P.F. 1960. Na, Cl, and water transport by rat ileum in vitro. *J. Gen. Physiol.* **43**:1137

Curran, P.F., Schultz, S.G. 1968. Transport across membranes: General principles. *In:* Handbook of Physiology. Sect. 6, Alimentary Canal. Vol. 3, p. 1217. American Physiological Society, Washington

Curran, P.F., Schwartz, G.F. 1960. Na, Cl and water transport by rat colon. *J. Gen. Physiol.* **43**:555

Curran, P.F., Solomon, A.K. 1957. Ion and water fluxes in the ileum of rats. *J. Gen. Physiol.* **41**:143

De Camilli, P., Peluchetti, D., Meldolesi, J. 1974. Structural difference between luminal and lateral plasmalemma in pancreatic acinar cells. *Nature (London)* **248**:245

De Camilli, P., Peluchetti, D., Meldolesi, J. 1976. Dynamic changes of the luminal plasmalemma in stimulated parotid acinar cells. A freeze-fracture study. *J. Cell Biol.* **70**:59

Diamond, J.M. 1962. The mechanism of solute transport by the gallbladder. *J. Physiol. (London)* **161**:474

Dunham, P.B., Hoffman, J.F. 1971. Active cation transport and ouabain binding in high potassium and low potassium red blood cells of sheep. *J. Gen. Physiol.* **58**:94

Dutta, S., Marks, B.H. 1969. Factors that regulate ^{3}H-ouabain accumulation by the isolated guinea pig heart. *J. Pharmacol. Exp. Ther.* **170**:318

Eigler, J., Crabbé, J. 1969. Effects of diuretics on active sodium transport in amphibian membranes. *In:* Renal Transport and Diuretics. K. Thurau and H. Jahrmarker, editors. p. 195. Springer-Verlag, Berlin

Ellory, D.C., Keynes, R.D. 1969. Binding of triated digosin to human red cell ghost. *Nature (London)* **221**:776

Erlij, D., Martínez-Palomo, A. 1978. Role of tight junctions in epithelial function. *In:* Membrane Transport in Biology. G. Giebisch, D.C. Tosteson, and H.H. Ussing, editors. Vol. 3, p. 27. Springer-Verlag, Berlin

Ernst, S.A., Mills, J.W. 1977. Basolateral plasma membranes localization of ouabain sensitive sodium transport sites in the secretory epithelium of the avian salt gland. *J. Cell Biol.* **75**:74

Field, M., Fromm, D., McColl, I. 1971. Ion transport in rabbit ileal mucosa. I. Na and Cl fluxes and short-circuit current. *Am. J. Physiol.* **220**:1388

Frederiksen, O., Leyssac, P.P. 1977. Effect of cytochalasin B and dimethylsulfoxide on isosmotic fluid transport by rabbit gallbladder "in vitro". *J. Physiol. (London)* **265**:103

Gabbiani, G., Chaponnier, C., Zumbe, A., Vassalli, P. 1977. Actin and tubulin co-cap with surface immuno globulins in murine B lymphocytes. *Nature (London)* **269**:695

Galli, P., Brenna, A., De Camilli, P., Meldolesi, J. 1976. Extracellular calcium and the organization of tight junction in pancreatic acinar cells. *Exp. Cell Res.* **99**:178

Grinstein, S., Erlij, D. 1974. Insulin unmasks latent sodium pump sites in frog muscle. *Nature (London)* **251**:57

Hoffman, J.F. 1969. The interaction between ^{3}H-ouabain and the Na-K pump in red blood cells. *J. Gen. Physiol.* **54**:343*s*

Hogben, C.A.M. 1955. Active transport of chloride by isolated frog gastric epithelium origin of the gastric mucosal potential. *Am. J. Physiol.* **180**:641

Joiner, C.M., Lauf, P.K. 1978. The correlation between ouabain binding and potassium pump inhibition in human and sheep erythrocytes. *J. Physiol. (London)* **283**:155

Koch, L.E.G., Smith, M.J. 1978. An association between actin and the major histocompatibility antigen H-2. *Nature (London)* **273**:274

Kyte, J. 1976. Immunoferritin determination of the distribution of $(Na^+ + K^+)$ ATPase over the plasma membranes of renal convoluted tubules. II. Proximal segment. *J. Cell Biol.* **68**:304

Landowne, D., Ritchie, J.M. 1970. The binding of triated ouabain to mammalian nonmyelinated nerve fibres. *J. Physiol. (London)* **207**:529

Leighton, J., Brada, Z., Estes, L., Justh, G. 1969. Secretory activity and oncogenicity of a cell line (MDCK) derived from canine kidney. *Science* **163**:472

Machen, T.E., Erlij, D., Wooding, F.B.P. 1972. Permeable junctional complexes. The movement of lanthanum across rabbit gallbladder and intestine. *J. Cell Biol.* **54**:302

Madin, S.H., Darby, N.B. 1958. As catalogued in: American Type Culture Collection Catalogue of strains. (1975) Vol. 2, p. 47. H.O. Hatt, editor. Washington, D.C.

Martínez-Palomo, A., Chávez, B., González-Robles, A. 1978. The freeze-fracture technique: Application to the study of animal plasma membranes. *In:* Electron Microscopy 1978. J.M. Sturges, editor. Vol. 3, p. 503. Microscopy Society of Canada, Toronto

Martínez-Palomo, A., Erlij, D. 1973. The distribution of lanthanum in tight junctions of the kidney tubule. *Pfluegers Arch.* **343**:267

Meldolesi, J., Castiglioni, G., Parma, R., Nassivera, N., De Camilli, P. 1978. Ca^{++}-dependent disassembly and reassembly of occluding junctions in guinea pig pancreatic acinar cells. Effect of drugs. *J. Cell Biol.* **79**:156

Meza, I., Sabanero, M., Martínez-Palomo, A., Cereijido, M. 1978. Relationship between tight junctions and cytoskeleton in monolayers of MDCK cells. *J. Cell Biol.* **79**:243*a*

Mills, J.W., Ernst, S.A. 1975. Localization of sodium pump sites in frog urinary bladder. *Biochim. Biophys. Acta* **375**:268

Mills, J.W., Ernst, S.A., DiBona, D.R. 1977. Localization of Na^+ pump sites in frog skin. *J. Cell Biol.* **73**:88

Misfeldt, D.S., Hamamoto, S.T., Pitelka, D.R. 1976. Transepithelial transport in cell culture. *Proc. Nat. Acad. Sci. USA* **73**:1212

Moore, P.B., Ownby, C.L., Carraway, K.L. 1978. Interactions of cytoskeletal elements with the plasma membrane of sarcoma 180 Ascites tumor cells. *Exp. Cell Res.* **115**:331

Nicolson, G.L. 1976. Transmembrane control of the receptors on normal and tumor cells. I. Cytoplasmic influence over cell surface components. *Biochim. Biophys. Acta* **457**:58

Oken, D.E., Whittembury, G., Windhager, E., Solomon, A.K. 1963. Single proximal tubules of *Necturus* kidney. V. Unidirectional sodium movement. *Am. J. Physiol.* **204**:372

Osborn, M., Born, T., Koitsch, H.J., Weber, K. 1978. Stereo immunofluorescence microscopy. I. Three dimensional arrangement of microfilaments, microtubules and tonofilaments. *Cell* **14**:477

Osborn, M., Weber, K. 1977. The display of microtubules in transformed cells. *Cell* **12**:561

Pisam, M., Ripoche, P. 1976. Redistribution of surface macromolecules in dissociated epithelial cells. *J. Cell Biol.* **71**:907

Quinton, P.M., Wright, E.M., Tormey, J. 1973. Localization of sodium pumps in the choroid plexus epithelium. *J. Cell. Biol.* **58**:724

Rabito, C.A., Tchao, R., Valentich, J., Leighton, J. 1978. Distribution and characteristics of the occluding junctions in a monolayer of a cell line (MDCK) derived from canine kidney. *J. Membrane Biol.* **43**:351

Rindler, M.J., Saier, M.H., Jr. 1978. An electroneutral exchange carrier for sodium in a dog kidney epithelial cell line (MDCK). *Int. Congr. Nephrol.* **7**:22 (*Abstr.*)

Rodríguez-Boulan, E., Sabatini, D.D. 1978. Asymmetric budding of viruses in epithelial monolayers: A model system for study of epithelial polarity. *Proc. Nat. Acad. Sci. USA* **75**:5071

Rozengurt, E., Heppel, L.A. 1975. Serum rapidly stimulates ouabain-sensitive $^{86}Rb^+$ influx in quiescent 3T3 cells. *Proc. Nat. Acad. Sci. USA* **72**:4492

Sachs, J.R. 1977. Kinetic evaluation of the Na-K pump reaction mechanism. *J. Physiol. (London)* **273**:489

Schultz, S.G., Zalusky, R. 1963. Ion transport in isolated rabbit ileum. I. Short circuit current and Na fluxes. *J. Gen. Physiol.* **47**:567

Shelanski, M., Gaskin, F., Cantor, C.R. 1973. Microtubule assembly in the absence of added nucleotides. *Proc. Nat. Acad. Sci. USA* **70**:765

Smith, J.B., Rozengurt, E. 1978. Serum stimulates the Na^+, K^+ pump in quiescent fibroblasts by increasing Na^+ entry. *Proc. Nat. Acad. Sci. USA* **75**:(11)5560

Spudich, A.J., Watt, S. 1971. The regulation of rabbit skeletal muscle contraction. *Biol. Chem.* **246**:4866

Sunqvist, K.G., Ehrnst, A. 1976. Cytoskeletal control of surface membrane mobility. *Nature (London)* **264**:226

Taylor, A., Mamelak, M., Goldbetz, H., Maffly, E. 1976. Evidence for involvement of microtubules in the action of vasopressin in toad urinary bladder. I. Functional studies on the effects of antimitotic agents on the response to vasopressin. *J. Membrane Biol.* **40**:213

Trupper, J.T., Zorgniotti, F., Mills, B. 1977. Potassium transport and content during G, and S phase following serum stimulation of 3T3 cells. *J. Cell Physiol.* **91**:429

Ussing, H.H., Andersen, B. 1955. The relation between solvent drag and active transport of ions. *Proc. Int. Congr. Biochem.* **3**:434

Wade, J.B., DiScala, V.A., Karnovsky, M.J. 1975. Membrane structural specialization of the toad bladder revealed by the freeze-fracture technique. I. The granular cell. *J. Membrane Biol.* **22**:385

Weber, K., Wehland, J., Herzog, W. 1976. Griseofulvin interacts with microtubules both *in vivo* and *in vitro*. *J. Mol. Biol.* **102**:817

Zadunaisky, J.A., Candia, O.A., Chiarandini, D.J. 1963. The origen of the short-circuit current in the isolated skin on the South American frog *Leptodactylus ocellatus*. *J. Gen. Physiol.* **37**:393

Received 10 April 1979; revised 28 August 1979